4-2-2014

Measuring soil frost depth in forest ecosystems with ground penetrating radar

John R. Butnor
USDA Forest Service, Southern Research Station, jbutnor@fs.fed.us

John L. Campbell
USDA Forest Service, Northern Research Station, jlcampbell@fs.fed.us

James B. Shanley
USGS, New England Water Science Center, jshanley@usgs.gov

Stanley J. Zarnoch
USDA Forest Service, Southern Research Station, szarnoch@fs.fed.us

Agricultural and Forest Meteorology 192–193 (2014) 121–131

Contents lists available at ScienceDirect

Agricultural and Forest Meteorology

journal homepage: www.elsevier.com/locate/agrformet

Measuring soil frost depth in forest ecosystems with ground penetrating radar

John R. Butnor[a,*], John L. Campbell[b], James B. Shanley[c], Stanley J. Zarnoch[d]

[a] USDA Forest Service, Southern Research Station, University of Vermont, 81 Carrigan Drive, Aiken Room 210, Burlington, VT 05405, United States
[b] USDA Forest Service, Northern Research Station, 271 Mast Road, Durham, NH 03824, United States
[c] USGS, New England Water Science Center, Vermont Office, Montpelier, VT 05602, United States
[d] USDA Forest Service, Southern Research Station, Clemson University, SC 29634, United States

ARTICLE INFO

Article history:
Received 8 November 2013
Received in revised form 7 February 2014
Accepted 7 March 2014
Available online 2 April 2014

Keywords:
GPR
Forest
Frozen soil
Nondestructive
Soil frost

ABSTRACT

Soil frost depth in forest ecosystems can be variable and depends largely on early winter air temperatures and the amount and timing of snowfall. A thorough evaluation of ecological responses to seasonally frozen ground is hampered by our inability to adequately characterize the frequency, depth, duration and intensity of soil frost events. We evaluated the use of ground penetrating radar to nondestructively delineate soil frost under field conditions in three forest ecosystems. Soil frost depth was monitored periodically using a 900 MHz antenna in South Burlington, Vermont (SB), Sleepers River Watershed, North Danville, Vermont (SR) and Hubbard Brook Experimental Forest, New Hampshire (HBEF) during winter 2011–2012 on plots with snow and cleared of snow. GPR-based estimates were compared to data from thermistors and frost tubes, which estimate soil frost depth with a color indicating solution. In the absence of snow, frost was initially detected at a depth of 8–10 cm. Dry snow up to 35 cm deep, enhanced near-surface frost detection, raising the minimum frost detection depth to 4–5 cm. The most favorable surface conditions for GPR detection were bare soil or shallow dry snow where frost had penetrated to the minimum detectable depth. Unfavorable conditions included: standing water on frozen soil, wet snow, thawed surface soils and deep snow pack. Both SB and SR were suitable for frost detection most of the winter, while HBEF was not. Tree roots were detected as point reflections and were readily discriminated from continuous frost reflections. The bias of GPR frost depth measurements relative to thermistors was site dependent averaging 0.1 cm at SB and 1.1 cm at SR, and was not significantly different than zero. When separated by snow manipulation treatment at SR, overestimation of soil frost depth (5.5 cm) occurred on plots cleared of snow and underestimation (−1.5 cm) occurred on plots with snow. Despite some limitations posed by site and surface suitability, GPR could be useful for adding a spatial component to pre-installed soil frost monitoring networks.

Published by Elsevier B.V.

1. Introduction

Seasonal soil freezing is an important natural perturbation that is common in cold regions around the world. Soil frost depth can be highly variable and depends largely on early winter air temperatures and the amount and timing of snowfall. Recent interest in understanding soil freezing effects on ecological systems has stemmed from the expectation that future changes in climate will alter the temporal patterns and spatial extent of seasonally frozen ground (Brown and DeGaetano, 2011; Campbell et al., 2010; Henry, 2008). Changes in soil freezing regimes could have important implications for forest ecosystems, since freezing influences physical, chemical, and biological processes in soil (e.g., Groffman et al., 2001; Haei et al., 2011; Hentschel et al., 2009; Iwata et al., 2010). A number of studies over the last decade have shown that soil frost events influence soil carbon and nitrogen leaching from forested watersheds (e.g., Christopher et al., 2008; Fitzhugh et al., 2003; Groffman et al., 2011; Kaste et al., 2008; Matzner and Borken, 2008). However, a thorough evaluation of ecological responses to seasonally frozen ground is hampered by our inability to adequately characterize the frequency, depth, duration and intensity of soil frost events.

Soil frost is often considered problematic, and the heaving associated with it can have adverse effects, such as uplifting planted seedlings and compromising the integrity of roads and structures (Saarenketo and Scullion, 2000). In forest ecosystems, long-term observations and short-term experiments have shown that soil

* Corresponding author. Tel.: +1 440118026561719.
E-mail addresses: jbutnor@fs.fed.us (J.R. Butnor), jlcampbell@fs.fed.us (J.L. Campbell), jshanley@usgs.gov (J.B. Shanley), szarnoch@fs.fed.us (S.J. Zarnoch).

http://dx.doi.org/10.1016/j.agrformet.2014.03.005
0168-1923/Published by Elsevier B.V.

freezing can affect ecosystem processes by damaging fine roots (Tierney et al., 2001), and altering litter decomposition, trace gas fluxes, and nutrient leaching (Fitzhugh et al., 2003; Groffman et al., 1999, 2001, 2011). Soil frost can also alter hydrologic flow paths, particularly in agricultural areas where hard, impenetrable "concrete" frost forms (Shanley and Chalmers, 1999). There are some operational benefits of frost; frozen soil can improve accessibility and minimize disturbance during logging operations and loosen compacted agricultural soil.

Despite the importance of soil frost in ecological studies, the methods for measuring its depth are rudimentary and need improvement. One of the oldest methods is a direct measure that involves digging pits and visually detecting ice crystals or using tactile methods to determine whether the ground "feels" frozen (e.g., Campbell et al., 2010). This approach is subjective and destroys or impairs the experimental area and has largely been replaced by more favorable indirect methods such as frost tubes (Ricard et al., 1976), temperature probes and electrical methods. Frost tubes are a useful indicator of soil frost depth; but, they only provide data for specific points across the landscape and may exhibit lag effects during rapid changes in temperature (McCool and Molnau, 1984). Another common method uses temperature probes installed at fixed depths in the soil profile, and the interpolated 0 °C isotherm is considered the frost line. This method provides measurements over time when connected to a data logger; however, it requires pre-installation and is not well suited for measuring soil frost over broad areas. Additionally, it is possible that solutes may depress the freezing point of soils, especially in areas with environmental contaminants (e.g., road salt) and the gradient between temperature probes in the profile is assumed to be linear, which may be incorrect. Other, more technologically advanced methods of soil frost measurement such as time domain reflectometry and electrical conductance have similar limitations (Baker et al., 1982; Hayhoe and Balchin, 1986). Ground penetrating radar (GPR) is also becoming recognized as a useful tool for quantifying soil frost (Steelman and Endres, 2009; Steelman et al., 2010) and has advantages over conventional methods. It may be rapidly deployed and provides spatially contiguous frost depth detection; series of parallel transects may be arranged to collect frost depth data over broad areas.

GPR antennas propagate short pulses of electromagnetic energy into the ground and receive reflected signals on the soil surface. Whenever a pulse contacts an interface separating layers with different electrical conductance, a portion of the energy is reflected back to a receiver on the surface. The material property that creates the electromagnetic contrast and causes reflections is relative dielectric permittivity (ε_r), which is a dimensionless quantity relating to a material's behavior when subjected to an electric field. The larger the difference between the dielectrics of two adjacent materials, the stronger the radar wave reflection. For example, ε_r of frozen soil varies from 2 to 8, while moist soils range from 10 to 30 (Cassidy, 2009). When freshwater freezes, ε_r drops from 81 to 4 (air = 1); a phenomenon that makes it possible to detect frozen layers with GPR (Daniels, 2004). If GPR emerges as a reliable tool for quantifying soil frost quickly and accurately over plots or broader areas, it could be an integral part of focused ecological response studies, or used in conjunction with established frost networks to aid in the interpretation of long-term biogeochemical patterns.

The purpose of this study was to evaluate the suitability of GPR for characterizing soil frost in forest ecosystems in northern New England. While it is possible to detect frost depth with GPR, there are a number of uncertainties that need to be resolved to use the tool effectively in forest ecosystem research applications and routine monitoring. Earlier studies were limited to agricultural lands where snow cover was removed immediately before scanning to improve contact with the soil (Steelman and Endres, 2009; Steelman et al., 2010). However, snow removal is not ideal for monitoring protocols because it is labor intensive, causes disturbance, and enhances soil frost penetration. To date, GPR has not been deployed to assess soil frost depth in forests under native snow/surface conditions and there is no guidance as to productive approaches or suitability to enhance current monitoring protocols. The objectives of this study are to: (1) Determine if GPR can provide soil frost depth estimates comparable to those collected with thermistors and frost tubes, under varied site conditions common to New England forests (e.g., variable soils, topography, presence of rocks and tree roots), (2) Determine how the presence of snow cover affects frost depth detection, (3) Provide guidance on future applications of GPR to estimate soil frost depth in forests.

Fig. 1. Location of study sites in Vermont and New Hampshire, USA.

2. Materials and methods

2.1. Study sites

The study was conducted across an elevation gradient at three sites in northern Vermont and New Hampshire (Fig. 1). The South Burlington, Vermont (SB) site is a 25 year-old balsam fir (*Abies balsamea*) planation adjacent to the USDA Forest Service, Northern Research Station Laboratory, 95 m a.s.l., 44.45338° N–73.19088° E. The moderately well drained soil is loamy sand with few pebbles in the upper 0.5 m. The Hubbard Brook Experimental Forest (HBEF) site in Thornton, New Hampshire, is a mature northern hardwood stand, 290 m a.s.l., 43.94648° N–71.70153° E. The soil is loamy sand with some rocks in the upper 0.5 m and is well-drained. The Sleepers River Watershed (SR), North Danville, VT, site is a naturally regenerated balsam fir stand with trees >40 years old, 590 m a.s.l., 44.4854° N–72.16669° E. The soil is sandy loam with numerous rocks in the upper 0.5 m and somewhat poorly drained. Soil texture and organic matter (OM) content for each site is presented in Table 1.

2.2. Experimental design and snow depth manipulation

A randomized complete block design where snow manipulation (snow removed, snow intact) was replicated three times was used to implement the study and analyze data at each site (SB, HBEF, SR). Within a replicate, one plot (2 m × 10 m) was shoveled free of snow each week and snow cover was left intact on the other (2 m × 10 m) for a total of 6 plots per site. The snow removal treatment had two

Table 1
Mean percent soil parameters in the upper 30 cm at study sites.

	South Burlington, Vermont	Sleepers River, Vermont	Hubbard Brook, New Hampshire
Sand	77.5	58.4	80.5
Silt	20.8	38.0	18.8
Clay	1.7	3.6	0.7
OM	4.0	10.9	11.0

purposes: to create areas of deeper soil frost penetration and to make comparative assessments of frost depth delineation through snowpack with the snow covered plots. Prior studies of soil frost detection by GPR were on soils shoveled free of snow (Steelman and Endres, 2009; Steelman et al., 2010), hence the ability to detect seasonal soil frost through snow is unknown.

2.3. Frost tubes

Frost tubes were constructed as described by Ricard et al. (1976), where a polyethylene tube is filled with a 0.05 percent solution of methylene blue dye and inserted into a PVC pipe installed vertically in the soil to a depth of 1 m. As the solution freezes, the dye is excluded from the ice, creating a discrete line of demarcation between the frozen (clear) and liquid (blue) portions. The tube is removed from the PVC pipe to measure the depth of frozen solution, yielding an estimate of the frost depth of the surrounding soil. Frost tubes were installed in the center of each 2 m × 10 m plot at 1, 3, 5, 7, and 9 m. At each site, a total of 30 frost tubes were installed (6 plots × 5 tubes).

2.4. Soil thermistors

At each site, thermistors with an accuracy of ±0.2 °C were used to measure air temperature and soil temperature at one snow removal plot and one snow plot. Soil temperature depth profiles were created by inserting the thermistors at depths of 1, 3, 5, 10, 15, 20, 25 cm in the snow removal plot and 1, 3, 5, 10, 15, 20 cm in the snow plot. These temperature measurements were logged continuously using Hobo U21-002 data loggers (Onset Computer Corp., Pocasset, MA). Interpolation between temperature probes was necessary to compute a zero degree isotherm (ZDI) and predict frozen conditions. Though buried thermistors that give instantaneous soil temperature readings are not "direct" indicators of soil freezing per se, they were used as a point of reference to compare frost depth estimates from GPR surveys and frost tubes.

2.5. GPR

The basic principles and theory of frost detection with GPR are well described by Steelman and Endres (2009) and Steelman et al. (2010). In the field, GPR transect data are collected in reflection mode by pushing the antenna across the ground in a cart or sled (Fig. 2) configuration. The antenna propagates an electromagnetic wave into the ground or snow and receives waves reflecting off soil layers and objects with contrasting dielectric properties. The data are comprised of two-way travel time and signal amplitude. Depth is calculated using two-way travel time and the ε_r of the soil transited (Steelman and Endres, 2009). Steelman and Endres (2009) and Steelman et al. (2010) used the common mid-point (CMP) sounding method to determine ε_r of soil layers by depth. The CMP method involves separating the GPR transmitter (T_x) and receiver (R_x), then collecting one-way travel time and amplitude data between them across a range of distances around a common mid-point e.g., 0.02 m steps along a 2 m transect (Steelman and Endres, 2009). CMP soundings are time consuming and give information for a small area compared to a transect. Preliminary testing of CMP soundings at SR and HBEF showed that variable frost depth, snow depth, point reflections from rocks and tree roots, uneven topography and disturbance of snow introduced too much error to calculate vertical distribution of soil ε_r.

In the present study, ε_r was measured at each site by scanning a calibration transect where reference reflectors (aluminum rods) were horizontally inserted into undisturbed soil at depths of 10, 20, and 30 cm. The two-way travel time between the ground surface and each of the reflectors was used to determine ε_r of frozen and unfrozen soil and accurately characterize velocity (depth) on a given day. This approach is a simpler means of determining ε_r of frozen soil than CMP sounding, but only provides the mean ε_r to the reflector versus a profile where ε_r can vary with depth.

All GPR data were collected with a SIR-3000 radar unit (Geophysical Survey Systems Inc. (GSSI), Salem, NH) equipped with a 900 MHz antenna in reflection mode. Prior to snow accumulation, the plots were surveyed with a three wheeled survey cart equipped with an integrated survey wheel encoder which meters out electromagnetic pulses for the distance traveled (i.e. 100 pulses/m). Every 0.01 m, a reflection trace or waveform comprised of the amplitude of reflected energy and the two-way travel time was collected. These waveforms were stacked to create a radargram, which is a two dimensional profile of reflection data (amplitude and depth to reflection) across a given distance. The data were recorded in standard GSSI format (*.dzt). Once snow accumulated, a customized sled was used to measure the plots (Fig. 2). Since the survey wheel cannot be used in snow, the SIR-3000 was set to time mode, the sled was advanced at an even pace and electronic reference marks were tagged to the data at fixed intervals. Gain settings (2 or 3 point) were adjusted each day to optimize the detection snow/soil and frozen/unfrozen soil interfaces in real-time.

Minimal post-collection data processing was needed, since the collection parameters were optimized in the field for real time viewing. Radan 7.0 software (Geophysical Survey Systems Inc., Salem, NH) was used to correct the position and vertical scaling (depth) using field-determined dielectric values. When "ringing"

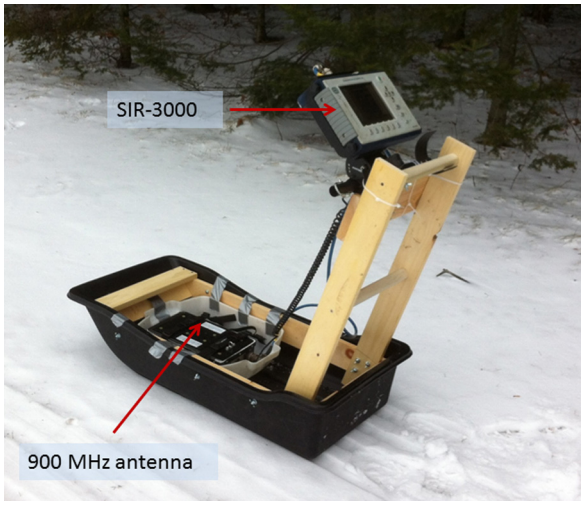

Fig. 2. Sir-3000 GPR unit and 900 MHz antenna configured in a custom sled for travel over snow.

noise was induced in the GPR data by wet surface conditions, it appeared as broad horizontal reflections that interfered with the frost delineation. Background removal processing was used to remove instances of mild ringing on a few radargrams. Display gain was added to detect faint frost reflections and "interactive interpretation" (a process in Radan 7.0) was employed to highlight frost depth and output depth of frost detection in a semi-automated manner.

2.6. Periodic sampling

The SB site was sampled 12 times with GPR due to ready access near the Forest Service Laboratory, while the SR and HBEF sites were each sampled five times during winter 2011–2012. The purpose of more frequent sampling at SB was to capture frost dynamics during transition periods (e.g., snow events, deep freezes, thaws and rain events) when possible. To scan a plot, the GPR sled was pushed across the calibration transect to profile the buried reflectors. Next, the sled was pushed through each plot, and when the midpoint of the antenna passed each frost tube an electronic mark was tagged to the GPR profile, allowing precise comparisons of GPR and frost tube estimates. Each frost tube was measured manually and the soil thermistor logger was downloaded at the time of the GPR survey. Snow depth was measured adjacent to each frost tube (5 per plot) with a meter stick. Frost tubes and snow depth were sampled weekly.

2.7. Method of analysis

All three measures of frost depth used in this study, ZDI, GPR and frost tubes are considered to be indirect measurements; there is no true value to compare them to. Observations collected with GPR and frost tubes were compared to the ZDI at a common location to quantify differences using the statistical criteria of bias, variance and accuracy using an approach modified from Zarnoch and Dell (1985). Bias is defined as average amount an estimate will vary from the true frost depth; it can be positive indicating an overestimate or negative for underestimates,

$$\text{Bias} = \sum_{i=1}^{n} \frac{\hat{\alpha}_i - \alpha}{n}$$

where, n sample size; α true value of frost depth; $\hat{\alpha}_i$ estimate of frost depth i ($i = 1, 2, 3, \ldots, n$)

While the true frost depth value is unknown, bias of GPR and frost tubes are presented relative to the ZDI. Variance is an estimate of precision and describes how much observations vary from their mean, rather than the true value,

$$\text{Variance} = \sum_{i=1}^{n} \frac{\left(\hat{\alpha}_i - \sum_{i=1}^{n} \frac{\hat{\alpha}_i}{n}\right)}{n}$$

The combined influence of bias and variance as represented by the mean square error, describes the difference between the estimator and the true value of frost depth, providing a measure of accuracy:

$$\text{M.S.E.} = \sum_{i=1}^{n} \frac{(\hat{\alpha}_i - \alpha)^2}{n}$$

Given that the zero degree isotherm represents a small sample size, the same approach was applied to quantify bias in GPR frost depth relative to frost tube estimates. This does not imply that frost tubes are a standard or reference, but they have been deployed for long term research at SR since 1986 and give context to GPR estimates.

Frost depth estimated by frost tubes and GPR (y axis) was plotted against frost depth derived from thermistors (x axis) at each site along with linear regression lines. To assess whether the lines are different from each other, a test of conditional error was used to determine if the slopes and intercepts were simultaneously equal (Miliken and Johnson, 1984) using a statistical approach described by Zarnoch (2009) and implemented with SAS 9.1 software (SAS Institute Inc., Cary, NC) using the general linear models procedure (PROC GLM). The hypothesis that "all slopes and all intercepts are equal" for a set of regressions was rejected if $p \leq 0.05$. If rejected, then contrasts were developed to compare all pairs of regression lines using the Bonferroni adjustment where a pair of regression lines was considered significant if the p-value was $\leq 0.05/$(number of comparisons within a set) (Zarnoch, 2009). The 95% confidence intervals for the intercept and slope parameters were compared to the 1:1 line to determine if they contained the intercept = 0 and slope = 1 values, respectively (PROC REG; SAS institute, Cary, NC) thereby establishing if they are different from ZDI. A similar regression analysis was used to compare plot-level mean frost depth estimated with GPR and frost tubes by site and snow treatment (i.e. ambient snow, snow removal). The effects of snow treatment, method (GPR, frost tubes) and sampling date (5 dates) on estimated frost depth were analyzed using a repeated measures analysis with the ar(1) covariance structure since the dates were approximately equally distant (PROC MIXED; SAS institute, Cary, NC).

3. Results

3.1. Field conditions during winter 2011–2012

Daily air and soil temperatures at 5 cm in snow and snow removal plots are presented in Fig. 3 and summarized on a monthly basis in Table 2. For the 5-month duration of the experiment, mean air temperature followed the elevation gradient: SB (2.6 °C), HBEF (0.3 °C), SR (−2.6 °C). Winter 2011–2012 was exceptionally mild in northern New England with low snowfall, numerous thaws and rain events, and observed air temperatures that were warmer than the 19-year average: SB (+4.0 °C), HBEF (+1.8 °C), SR (+1.8 °C). Monthly snow depth recorded at nearby stations was lower than historical averages for all months during the experiment (Table 2), SB was 10%, HBEF 13% and SR 48% of the 19 year mean. SB had no measurable snow accumulation beneath the dense balsam fir canopy (Table 2).

3.2. Frost detection and interpretation with GPR

Prior to the development of frost, radargrams show roots and rocks as discrete reflection hyperbolas. Soil frost, abrupt changes in soil horizons or moisture content may appear as continuous, horizontal reflections. The detection of a soil frost line with GPR requires interpretation made by an experienced operator. A series of radargrams and selected waveforms collected one month apart at SB are presented to highlight key interpretative features (Fig. 4). As the soil begins to freeze, a diffuse horizontal reflection appears below and parallel to the ground surface on the radargram (Fig. 4A). The associated waveform shows a small peak below the ground wave reflection (Fig. 4A) and the frost tube indicates an initial detection of soil frost depth at 9 cm. On all three sites with snow removed, measuring on bare soil, soil frost was initially detected at depths of 8–10 cm. Reflections from tree roots are visible on the right side of the radargram. As the depth of frozen soil increases, the band of frost parallel to the surface becomes more apparent and the amplitude of the frost peak below the ground wave increases (Fig. 4B). Tree roots appear as simple reflection hyperbolas and are distinct from the frost detection. When the frost depth increases to

Table 2
Mean monthly temperature and snow depth statistics at the study sites during winter 2011–2012 and 19 year mean values from nearby recording stations.

Site	Month	2011–2012				19-year mean		
		Air temp. (°C)	Soil temp. at 5 cm (°C)	Max. snow cover (cm)	Mean snow cover (cm)	Air temp. (°C)	Max. snow cover (cm)	Mean snow cover (cm)
SB	December	−0.4	2.0	0	1[a]	−2.8[a]	na	8[a]
	January	−3.9	−1.2	0	3[a]	−7.0[a]	na	14[a]
	February	−2.0	−1.1	0	1[a]	−5.5[a]	na	17[a]
	March	5.6	2.7	0	1[a]	0.0[a]	na	11[a]
	April	7.3	5.5	0	0[a]	7.0[a]	na	1[a]
SR	December	−4.3	1.1	5	9[b]	−6.2[b]	33[b]	22[b]
	January	−8.1	0.1	30	28[b]	−10.1[b]	55[b]	42[b]
	February	−6.0	0.1	29	48[b]	−8.3[b]	68[b]	61[b]
	March	1.0	1.2	28	32[b]	−2.9[b]	77[b]	61[b]
	April	4.6	4.4	0	0[b]	3.8[b]	37[b]	19[b]
HBEF	December	−2.3	0.2	6	1[c]	−3.3[c]	20[c]	13[c]
	January	−5.0	−1.7	13	7[c]	−6.8[c]	34[c]	24[c]
	February	−2.6	−0.6	14	12[c]	−5.1[c]	42[c]	34[c]
	March	3.5	1.4	25	4[c]	−0.1[c]	38[c]	25[c]
	April	7.9	7.9	0	0[c]	6.1[c]	11[c]	4[c]

[a] Burlington International Airport (KBTV), NOAA, 5 km distant.
[b] Sleepers River Watershed, USGS, North Danville, VT, <1 km distant.
[c] Hubbard Brook Experimental Forest, USDA Forest Service, adjacent to site.

31 cm, the reflection continues to be distinct and some variation in frost penetration depth is noticeable along the length of the radargram (Fig. 4C). The waveform is characterized by a strong negative peak associated with frost (Fig. 4C). The amplitude of the peaks (phase changes) associated with the ground wave and the frost reflection are relatively high, making depth interpretation between them straightforward. The SB site experienced a rapid thaw in mid-March 2012 (Fig. 3) and the soil frost rapidly melted leaving behind saturated soils (Fig. 4D).

3.3. Site specific observations

Under suitable soil conditions, seasonal frost was routinely detected at depths of 10 cm or greater using a 900 MHz antenna. The best conditions for detection were snow-free, dry surface soils with minimal duff and debris. Tree roots and rocks presented as simple reflection hyperbolas and did not interfere with frost detection. The majority of the winter sampling days were suitable at SB (9 of 12 days) and SR (5 of 5 days), but not HBEF (2 of 5 days).

Uniform sandy loam soils with few surface obstructions made the SB site ideally suited for GPR. During the winter of 2011–2012, there were several rain events over frozen soil, and radargrams were un-interpretable when the soil surface was flooded or the near surface soil was saturated from thaw (Fig. 5). The SR soils were high in silt and often the water table was within 20–30 cm of the surface. Conditions were suitable for frost detection on bare soil and shallow snowpack on each of the five survey periods during the winter. The deepest snow cover encountered during the GPR surveys was ~35 cm and frost (if present) was detectable throughout the winter. Fig. 6 illustrates frost detection through snow. The reflection from soil frost was well defined where the snow was 20 cm deep (middle of radargram, below red arrow). As the snow gets deeper, the amplitude of the frost reflection declines. The amplitude of the reflection from the ground wave (air/snow interface) and the snow/soil interface was stronger than the frost reflection. Snow insulates the soil, protecting it from penetrating frosts and creating challenges for radar detection. Both shallow frost depth and deep snows result in faint reflections, complicating interpretation. In some instances the snow acted as an offset, lessening the destructive interference from the ground wave and allowing frost as shallow as 4–5 cm to be detected under shallow snow cover. Deeper snow resulted in fainter reflections from frost (Fig. 6), restricting conditions for detection to a narrow range of snow depth for the 900 MHz antenna used in this study.

The HBEF site had similar soil texture as SB in the upper 30 cm, but GPR performed poorly. There were many occasions where standing water or wet snow over frozen soil made radargrams un-interpretable either from excessive ringing noise or lack of a continuous reflection from the frozen/unfrozen interface. Due to the lack of snow cover, HBEF experienced record soil freezing; at one plot, frost was >60 cm deep. Once frost was deeper than 30 cm, it became undetectable at HBEF under otherwise suitable surface conditions (i.e. dry, bare surface), despite ready detection of frost depths >30 cm at SB and >40 cm at SR. Soil below 30 cm seemed much more coarse and granitic than at the other sites, but it was still surprising that frost detection would be so limited. Only two of five sample periods yielded useful GPR data due to the combination of unsuitable surface conditions and deep soil frost.

3.4. Bias, variance and accuracy of frost depth estimates

Using the ZDI as a point of reference for soil freezing, the bias, variance and accuracy of GPR and frost tube estimates were calculated for SB and SR (Table 3). The sample size is larger for frost tubes than GPR, since some additional sampling was done between GPR sampling intervals or when conditions were unsuitable for GPR. At HBEF, soil frost penetrated beyond the deepest thermistor (25 cm) in early January 2012, affording only one direct comparison with GPR and two with frost tubes (data not shown). When the snow cover and snow removal treatments were combined, bias was within 0.3 cm of ZDI for both GPR and frost tubes at SB. At SR, GPR overestimated frost depth by 1.1 cm and frost tubes overestimated by 2.9 cm relative to thermistor-derived data (Table 3). Due to a lack of snow cover at SB, there was no effective snow manipulation treatment; hence bias criteria are not presented by treatment. At SR, GPR overestimated frost depth on the snow removal treatment (+5.5 cm) and underestimated frost depth measured through snow (−1.5 cm). Frost tubes overestimated frost depth on both treatments, but the bias was similar, +2.1 cm in snow removal and +3.3 cm through snow. Both methods were more accurate at SB (GPR 5.9; frost tube 2.0) than SR (GPR 22.1; frost tube 12.7) and the

Table 3
Mean frost depth bias, upper and lower 95% confidence limits, variance and accuracy estimated with GPR and frost tubes versus the ZDI at SB and SR using all observations during winter 2011–2012. The snow removal and snow treatments are combined for SB since there was no snow accumulation.

Site	Method	Treatment	*n*	ZDI (cm)	Bias (cm)	Lower 95% C.L. for bias	Upper 95% C.L. for bias	Var.	Accuracy (M.S.E.)
SB	GPR	Remove + Snow	11	12.5	0.1	−1.7	1.7	5.8	5.9
	Frost Tube	Remove + Snow	19	8.4	−0.3	−1.0	0.4	1.9	2.0
SR	GPR	Remove + Snow	8	9.5	1.1	−3.0	5.2	20.8	22.1
	Frost Tube	Remove + Snow	18	7.9	2.9	1.8	4.0	4.3	12.7
SR	GPR	Remove	3	15.8	5.5	−1.1	12.1	4.7	35.1
		Snow	5	5.7	−1.5	−6.3	3.3	12.1	14.4
	Frost Tube	Remove	6	13.75	2.1	−0.3	4.4	4.2	8.5
		Snow	12	5.0	3.3	2.0	4.6	3.9	14.7

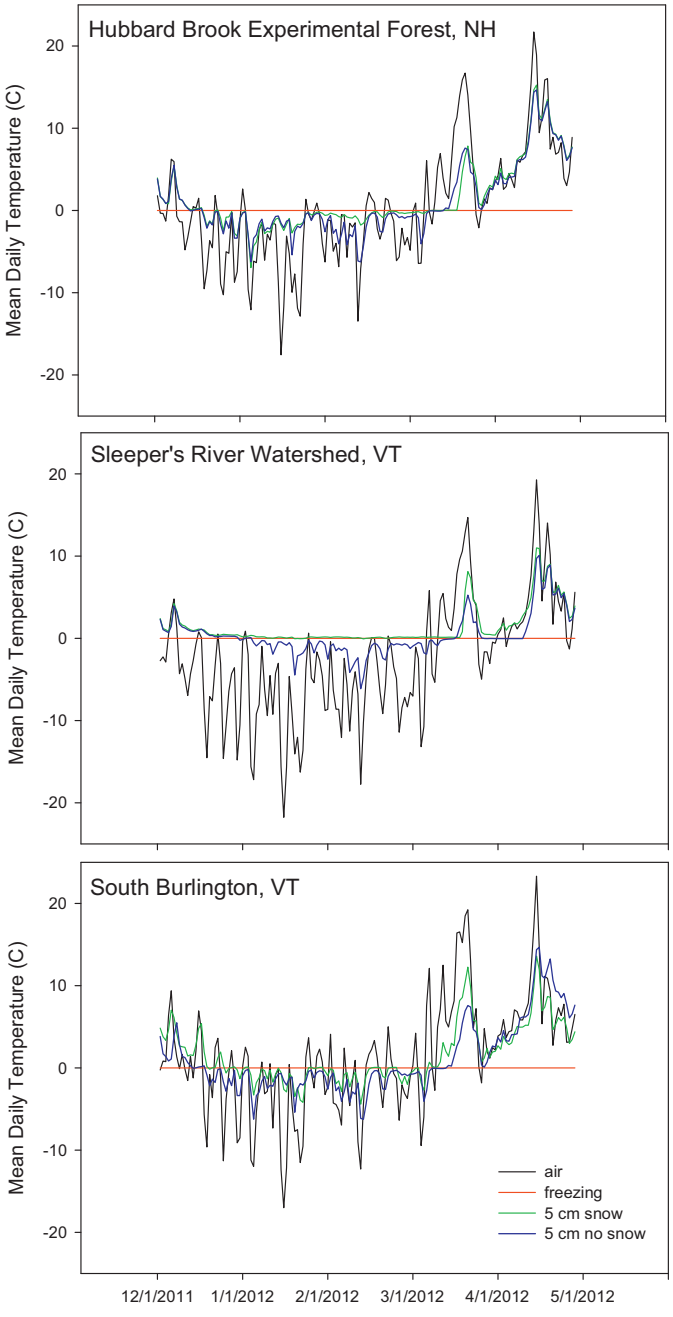

Fig. 3. Mean daily air and soil temperature (5 cm) temperatures during the 2011–2012 winter.

95% confidence interval for estimate bias included zero indicating that the bias was not significant.

Considering that the ZDI represents a small sample size and was limited to frost depths of 20 cm (snow) or 25 cm (removal), the same approach was applied to quantify bias, variance and accuracy of GPR frost depth estimates relative to frost tube estimates. At SB, GPR overestimated frost depth by 1 cm (Table 4). At SR, GPR overestimated frost depth in the snow removal treatment (3.9 cm)

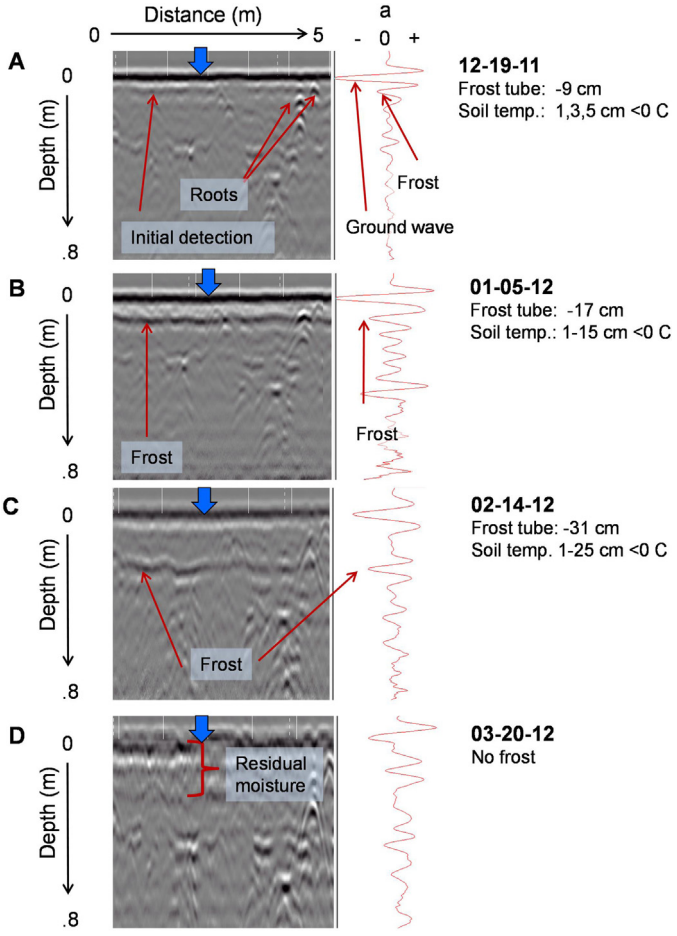

Fig. 4. Radargrams and selected waveforms showing progressive development of soil frost during the 2011–2012 at South Burlington, VT across four measurement periods. Frost detection is noted with red arrows on the radargram (left). Blue arrows note the location of the frost tube and the location where the waveform (red trace) was sampled from. The *x*-axis for the waveforms is relative amplitude ± (a). Frost depth measured with the frost tube and soil temperature data from thermistors collocated with the frost tube are presented on the right.

Table 4
Mean frost depth bias, variance and accuracy estimated with GPR versus frost tubes by site and treatment across all sample dates when soil frost was observed during winter 2011–2012. The number of sampling dates is *n* and the mean number of observations per date is in parenthesis.

Site	Treatment	*n* date (obs)	Frost tube depth (cm)	Bias (cm)	Lower 95% C.L. for bias	Upper 95% C.L. for bias	Var	Accuracy (M.S.E.)
SB	Remove + Snow	8(30)	18.5	1.0	−0.4	2.42	7.0	19.8
SR	Remove	5(15)	24.4	3.9	2.6	5.3	7.4	23.0
	Snow	5(15)	6.7	−2.5	−5.0	−0.1	12.3	26.5
HBEF	Remove	4(12)	30.5	−11.6	−16.4	−6.8	73.2	590.0
	Snow	4(10)	23.7	−5.9	−11.7	0	60.8	137.6
HBEF[a]	Remove	2(13)	21.6	−0.1	−2.7	2.5	14.1	32.6
	Snow	2(10)	20.6	1.0	−5.5	3.6	23.6	34.2

[a] Data from 1/04/2012 to 1/18/2012 only.

and underestimated in the snow treatment (−2.5 cm) similar to the trend observed with the ZDI data (Table 3). Surface conditions were frequently unsuitable for GPR at HBEF, using only the two sampling dates with favorable surface conditions; GPR exhibited negligible bias in the snow removal treatment and overestimated frost by 1 cm in the snow treatment (Table 4). GPR did not always detect deep frost at HBEF; the bias is the result of 'missed' soil frost later in the winter when frost level estimated with frost tubes exceeded 30 cm. Using only observations from 1/04/2012 to 1/18/2012 from plots with suitable surface conditions where frost had not exceeded 30 cm, the bias for HBEF was similar to observations at SB and SR.

3.5. Regression analysis of frost depth measured with GPR, frost tubes and thermistors

ZDI was used as a point of reference to compare frost depth estimates from GPR surveys and frost tubes at SR and SB (Fig. 7A and B). Due to limited GPR data, HBEF is not included. The hypothesis that the slopes and *y*-intercepts of the regression lines (GPR × thermistors and frost tubes × thermistors) are equal was rejected for SR ($F = 2.47$, $p = 0.03$), but not rejected for SB ($F = 0.48$, $p = 0.62$). Based on the 95% confidence limits, the *y*-intercept of SR frost tube was significantly different than 0, and the slopes and intercepts of the other regressions were not significantly different than the 1:1 line ($m = 1$, $b = 0$). Differences were observed at SR, where frost tubes indicated shallow frost when thermistors did not, indicating positive bias (Table 3).

Using plot level means (5 GPR and 5 frost tube estimates in each plot), GPR frost depth estimates were compared to those from frost tubes across all sites (Fig. 8A) and by the two snow manipulation treatments at SR (Fig. 8B). All suitable data from any date or treatment (HBEF $n = 6$; SB $n = 54$; SR $n = 30$) were used in these linear regressions (Fig. 8A), allowing for a much larger sample than the thermistor comparison in Fig. 7. We failed to reject the hypothesis that the slopes and *y*-intercepts of the regression lines (frost tubes × GPR) from all sites are equal ($F = 2.26$, $p = 0.07$). Since SB had no snow accumulation and HBEF had only one sampling date with complete data, the same analysis was run for SR by snow removal treatment (Fig. 8B). The hypothesis that the slopes and *y*-intercepts of the regression lines (frost tubes × GPR) from snow and snow removal treatments at SR are equal was rejected ($F = 21.11$, $p = 0.0001$). Using the 95% confidence limits, the *y*-intercept of SR snow removal was significantly different than the 1:1 line, while the slope was not.

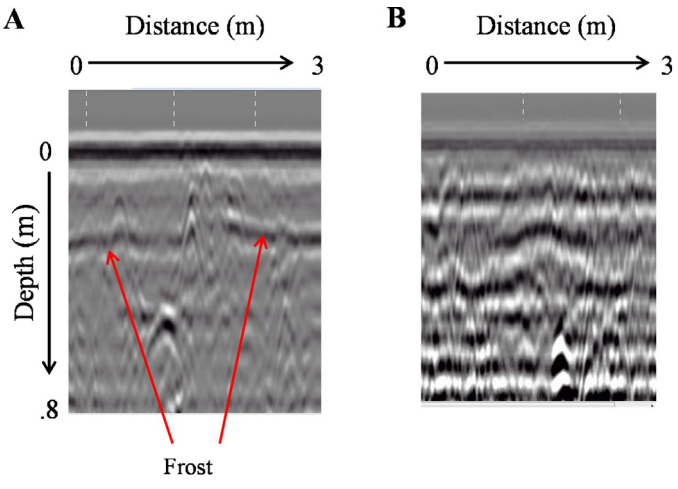

Fig. 5. Example of frost detection with GPR (28 cm deep) under favorable conditions at South Burlington, VT on January 23, 2012 (A) and a rain event the next day that interfered with GPR-based detection on January 24, 2012 (B).

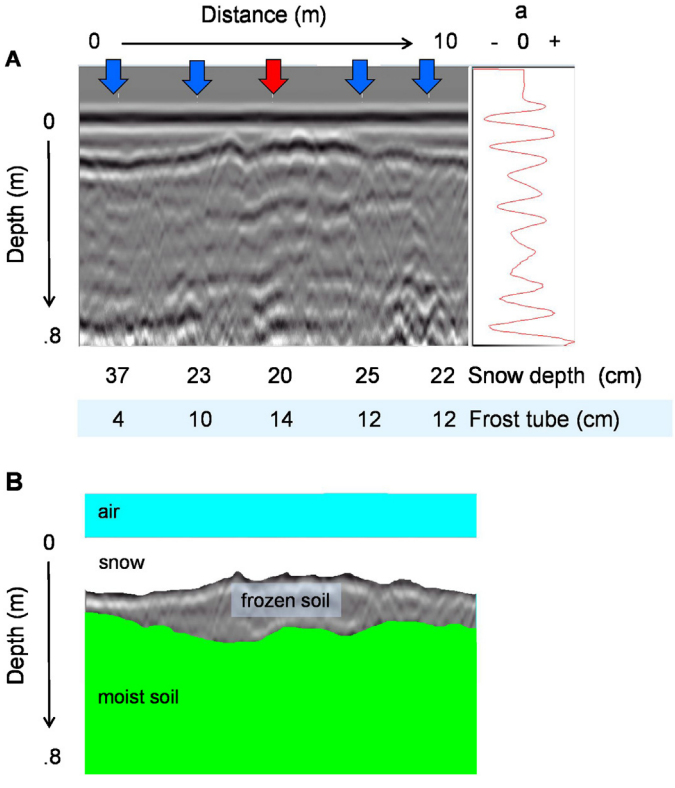

Fig. 6. Radargram collected along a 10 m transect at Sleepers River Watershed, over soils covered with 20–37 cm of snow on January 30, 2012 (A). Arrows indicate the location of frost tubes spaced 2 m apart and the red arrow shows where the waveform diagram on the right was collected. Below each arrow is the snow and frost depth collected at each frost tube. An interpretative schematic summarizing the features observable with GPR is also presented (B).

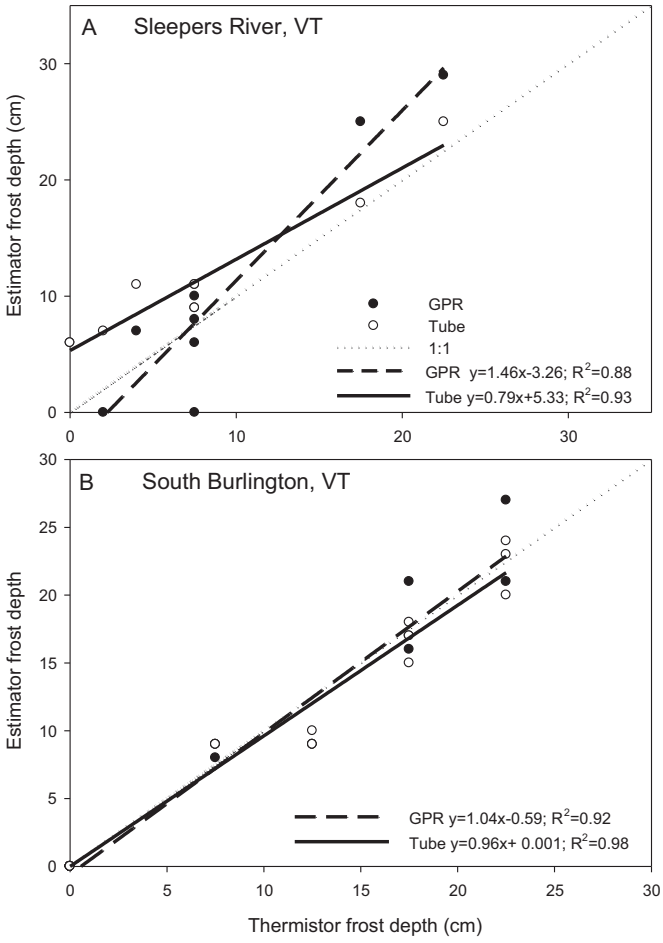

Fig. 7. Linear regression of GPR and frost tube depth estimates with data from thermistors buried at depths of 1, 3, 5, 10, 15, 20 and 25 cm at Sleepers River Watershed, VT (A) and South Burlington, VT (B).

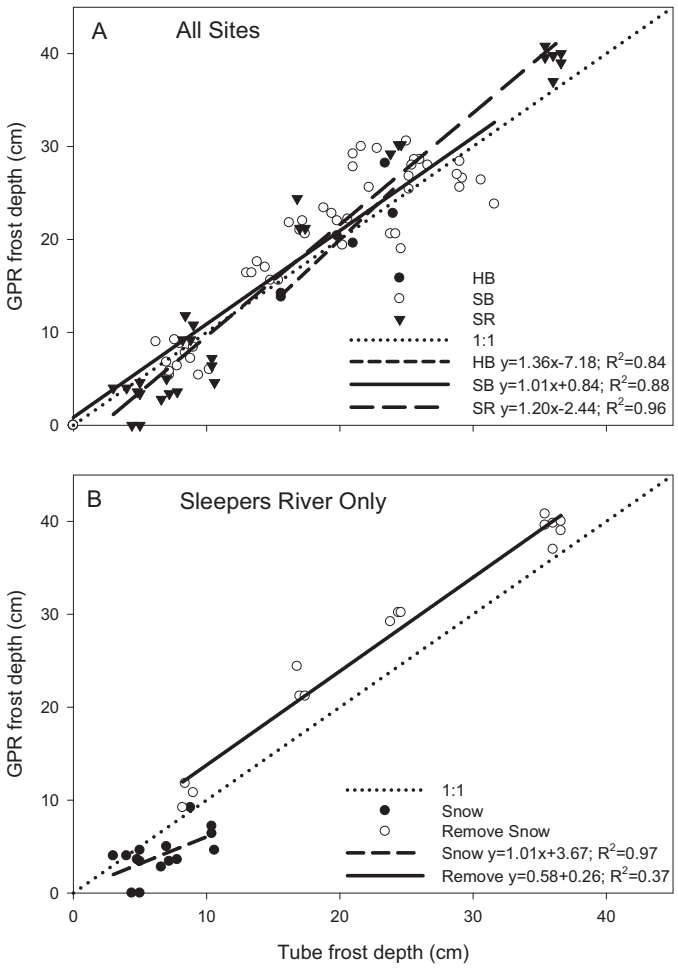

Fig. 8. Linear regression of frost depth estimated with GPR and frost tubes across all sites and treatments (A) and by snow manipulation treatment at Sleepers River Watershed, VT (B).

3.6. *Repeated measures of frost depth across snow manipulation treatments*

In early 2012, there were five periods when measurements of frost depth were conducted at each site within a week or less of each other (DOY 3–4, 17–18, 30 & 34, 46 & 51 and 66 & 73). Mean frost depths for each measurement method (GPR, frost tube) × snow manipulation treatment are plotted in Fig. 9. SR had the most snow cover throughout the study, HBEF gradually accumulated some snow and SB had no measurable snow (Table 2), leading to different soil frost treatment effects over time. As SB had no snow, there was no difference in frost depth between the snow and snow removal plots. At its peak in mid-February, frost penetration in the snow removal treatment was 17 cm deeper at HBEF and ~30 cm deeper at SR compared to the ambient snow plots (Fig. 9). The effect of method (GPR, frost tube), snow treatment (snow, snow removed) and measurement period (1–5) were analyzed using a repeated measures analysis (RMA) using the ar(1) covariance structure (Table 5). Measurement period had the largest effect on frost depth at each site as frost penetration progressed through DOY 73. At HBEF only one period (DOY 4) had a complete set of GPR data, so the method was dropped from the RMA. Snow treatment was not significant at HBEF and there was a treatment × period interaction (Table 5). Snow depth at HBEF was low during the first two sample periods, until accumulating snow insulated the forest floor later in the winter (Fig. 9). At SB there was no snow cover, hence no effect of snow treatment. While the main effect of method (GPR or frost tube) was not significant ($p = 0.63$), there was a method × period interaction ($p = 0.0001$). During period 2 (DOY 17) GPR recorded 3.8 cm greater frost depth than frost tubes, and during the other 4 periods there was no difference between methods (Table 6). Similarly at SR, the main effect of method was not significant ($p = 0.31$), but there was a treatment × method interaction ($p = 0.0033$). Method was analyzed separately by treatment; GPR estimated less frost depth in the snow treatment (−2.6 cm) and greater frost depth in the snow removal treatment (+3.9 cm) compared with frost tubes (Table 6) causing the interaction.

4. Discussion

When snow manipulation treatments were combined, both GPR and frost tube estimates of frost depth exhibited minimal bias relative to the ZDI and a high degree of accuracy at SB. At SR, when measurement methods were considered separately, GPR overestimated frost depth when snow was removed and underestimated it when snow was present. The number of observations at SB and SR are limited, but provide some insight into accuracy compared to ZDI for both techniques. When bias in GPR estimates is presented relative to frost tubes using 75 observations per treatment at SR, a similar pattern of overestimation for snow removal and underestimation for snow cover was observed. Average frost depth under snow at SR was only 6.7 cm; considering that GPR did not reliably detect frost from the surface to 4–5 cm depths on snow, any true frost depth less than 5 cm could be missed by GPR and reported

Table 5
Summary of repeated measures analysis degrees of freedom, *F* and *p*-values for the effects of measurement method (GPR, frost tube) and snow manipulation treatment on frost depth estimates across five sample periods in early 2012.

Source of variation	Numerator d.f.	HBEF		SB		SR	
		F	*p*-value	F	*p*-value	F	*p*-value
Treatment	1	2.75	0.1685				
Period	4	**46.07**	**0.0001**				
Treatment × Period	4	**15.96**	**0.0001**				
Treatment	1			0.44	0.5251	**307.48**	**0.0001**
Method	1			0.26	0.6253	1.28	0.3106
Treatment × Method	1			2.51	0.1488	**28.34**	**0.0033**
Period	4			**299.77**	**0.0001**	**159.90**	**0.0001**
Treatment × Period	4			0.45	0.7693	**125.78**	**0.0001**
Method × Period	4			**21.67**	**0.0001**	2.17	0.0984
Treatment × Method × Period	4			0.47	0.7570	1.40	0.2608

Significant effects and interactions (*p*-values ≤0.05) are highlighted.

Table 6
Least square means for illustrating the method * period interaction for South Burlington and the treatment * method interaction for Sleepers River. The *p*-value is based on an *F*-test for simple main effects of Method for each level of Period or Treatment using the slice option in SAS.

Method	South Burlington period					Sleepers treatment	
	1	2	3	4	5	Snow	Removal
GPR	7.3	21.9	20.6	28.5	27.0	4.1	28.3
Tube	8.9	18.1	21.8	26.8	27.2	6.7	24.4
p-Value	0.2254	0.0074	0.3748	0.1822	0.8325	0.0322	0.0064

as zero creating a negative bias. The cause of the systemic positive bias on the snow removal treatment at SR is likely the result of heterogeneous dielectric properties, both spatially and by depth. Using one calibration transect with buried reflectors to compute a simple mean dielectric was adequate at SB, but resulted in greater bias at SR. Sandy soils at SB were homogenous, well drained and devoid of rocks, while SR soils presented an electrically more complex profile i.e. variable drainage, many rocks and high silt content. If greater accuracy is needed, CMP soundings may be required to map dielectric changes in the soil profile (Steelman et al., 2010), despite issues due to factors such as uneven terrain and the presence of snow. There are no other reports that verify or corroborate seasonal frost detection with GPR with some other metric (temperature, physical observation) in the literature to compare to this study. GPR depth data are usually presented as two-way traveltimes, which can be used with the velocity profile or ε_r dynamics of the soil to determine the proper depth to some interface. The biophysical significance of bias relative to the true frost depth, is something that needs to be determined by researchers with their specific application in mind. For most applications, bias of 1 or 2 cm is minimal; whereas a larger bias of 3–5 cm might be acceptable for deep frost, but not for shallow frost.

Soil frost was detectable in forest soils and through shallow snow (<35 cm), though the specific site and surface conditions ultimately determined GPR suitability for any given sampling period. At SR and SB, even with some method bias (Table 3) and treatment effects, GPR and frost tube measurements were similar (Fig. 9). Where statistically significant differences were noted in the repeated measures analysis, further examination of the least square means for method * period and treatment * method showed the differences did not exceed 4 cm (Table 6) and could be combined to provide individual estimates for frost monitoring programs. GPR has the potential to sample larger areas and does not require preinstallation other than a calibration reflector for depth reference; however the technique is affected by surface conditions and cannot reliably estimate shallow frost that is < 8–10 cm (using 900 MHz antenna) on bare soil. Frost tubes are more reliable on a day-to-day basis while having similar accuracy. During periods of rapid thaw, we observed surface soils thaw and become saturated with water; under these conditions GPR did not give interpretable results, due to dispersive scattering of the electromagnetic waves in the wet soil. Consequently, frost tubes were suited to measuring frost depth at specific points, whereas GPR is useful for measuring it over broad areas when the conditions are suitable.

The inability of GPR to detect deep soil frost at HBEF under otherwise suitable surface conditions limited its utility. Range settings (ns) were increased to expand the detection depth and lower frequency antennas (400 MHz) were tested without success. Seasonal frost is known to inhibit infiltration in otherwise porous soils, enhancing spring runoff, but it also effectively cuts off inputs of surface water (French et al., 2006). A plausible explanation for the compromised results at HBEF is that seasonal frost made the well-drained, coarse soils impermeable to infiltration. Without replenishment of water from the surface, soil below the frost line became dry enough to have dielectric values similar to frozen moist soil, eliminating any detectable contrasts.

While snow and the near-surface soil were not the target of interest in this study and were viewed as a medium that needed to be transited to detect soil frost, their importance quickly became apparent. The success of using GPR to measure soil frost is dependent on the specific properties of snow and soil. The comparatively cold temperatures at SR resulted in a dry and low density (ε_r = 3.2–4) snowpack that was suitable for penetration with GPR. The dielectric properties of ice and snow depend on many factors, including density, temperature, moisture, ice crystal orientation, dissolved ions and free water content of the frozen substrate (Evans, 1965). At higher permittivity, surface snow and ice will cause signal attenuation and scattering, limiting the suitability of GPR for this application. Examples of less desirable surface conditions encountered during this experiment include: granular snow (ε_r = 15; Kopp, 1962), compact wet snow (ε_r = 50; Watt and Maxwell, 1960) and freshwater (ε_r = 81). The surface conditions that limited the utility of GPR at HBEF highlight the vulnerability of GPR to environmental conditions.

In cold regions, sub-freezing air temperatures and snow cover both influence soil frost dynamics (Decker et al., 2003; Yin and Arp, 1993). For a methodology to be thoroughly useful in ecological applications it should work through snow cover without

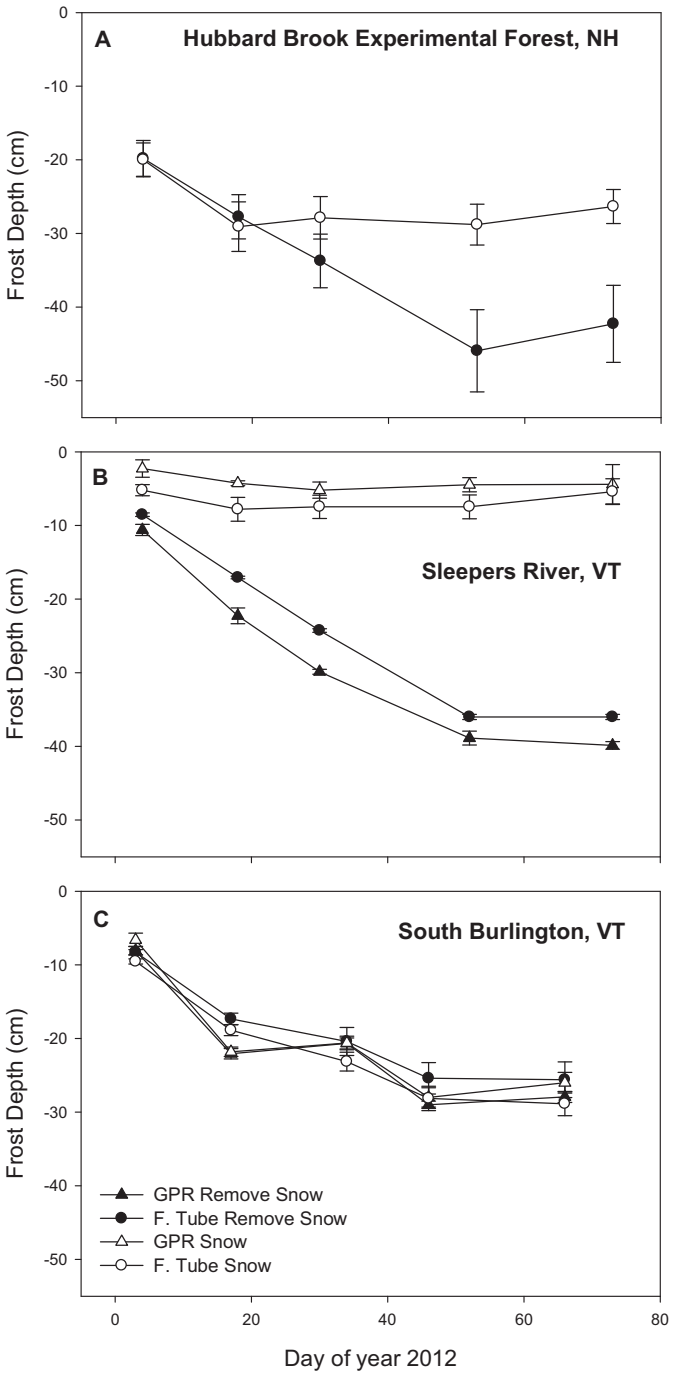

Fig. 9. Effect of snow manipulation and measurement method on estimated mean soil frost depth (± s.e.) over time.

disturbing its insulating properties. From observations at SR, detection through shallow snow (<35 cm) is possible if the soil frost is greater than 4–5 cm. Soil frost detection becomes problematic when the amplitude of the reflected energy from the air/snow and snow/frozen soil interfaces overwhelms the reflection of the frost/moist soil interface which typically has less contrast between ε_r values than the aforementioned interfaces and increased signal attenuation with depth. This is further complicated by shallow frosts with the close proximity of the frost/moist soil interface to the soil surface on snow covered plots. The deepest snows surveyed in this study were ~35 cm, and detection through deeper snow seems unlikely using a 900 MHz antenna, as frost reflections became increasingly faint the deeper the snow depth was. Lower frequency antennas (200–400 MHz) would be more capable of penetrating deep snow, but would not have the resolution to detect faint frost reflections and separate them from the snow/frozen soil interface. Others have been very successful using GPR to detect frost after snow removal (Steelman and Endres, 2009; Steelman et al., 2010). However, in ecological monitoring, snow removal is undesirable due to its impact on nutrient cycling, root health and possible tree mortality (e.g., Comerford et al., 2013; Schaberg et al., 2011). Tree roots are often more susceptible to freezing damage than more cold hardy above ground components (Tierney et al., 2001).

Based on this study there are a number of criteria that can be used to evaluate the potential applicability of GPR and enhance the implementation of GPR for soil frost sampling:

- Assess whether the minimum depth of frost detection of 8–10 cm on bare soil and 4–5 cm through snow is sufficient for the application.
- Determine if the potential method bias is within the bounds of monitoring goals.
- Select sites with soil conditions known to be suitable for GPR surveys, i.e. suitability maps (Doolittle et al., 2007).
- Anticipate that standing water on frozen soil, wet snow, surface thaw and deep snow pack will interfere with collection of GPR data in reflection mode.
- Depending on winter conditions, surfaces may not always be conducive to GPR surveys, if rigid weekly measurements are required, adequate coverage with thermistor profiles or frost tubes is needed.

5. Conclusions

In the absence of snow, frost was initially detected at 8–10 cm depth in the soil, dry snow up to 35 cm deep enhanced near-surface frost detection raising the minimum depth to 4–5 cm. Favorable surface conditions for GPR detection were bare soil or shallow dry snow where frost had penetrated to the minimum detectable depth. Unfavorable conditions included: standing water on frozen soil, wet snow, surface thaw and deep snow pack.

The bias of GPR frost depth measurements relative to Zero Degree Isotherm was site dependent averaging 0.1 cm at SB and 1.1 cm at SR, and was not different than zero using 95% confidence intervals. When separated by snow manipulation treatment at SR, overestimation (5.5 cm) occurred on plots cleared of snow and underestimation (−1.5 cm) snow plots. The bias of frost tube depth estimates relative to ZDI was also site dependent averaging −0.1 cm at SB and 2.9 cm at SR, however its bias was less affected by snow manipulation (2.1 cm, snow removal; 3.3 cm, undisturbed snow).

Winters with deep snow and shallow frost will make frost detection with GPR difficult, due to signal attenuation. Removal of snow simplified detection, though it significantly alters frost dynamics. Despite some limitations posed by site and surface suitability, GPR could be readily applied to add a broader spatial component to pre-installed soil frost monitoring networks.

Acknowledgments

This research was supported by a grant from the Northern States Research Cooperative, Theme Two: Sustaining Ecosystem Health in Northern Forests (http://nsrcforest.org), administered by the University of New Hampshire. We appreciate the technical assistance and field expertise provided by John Bennink, USDA Forest Service, Northern Research Station. We also appreciate advice on

field sampling and post-collection data processing offered by Brian Jones, Geophysical Survey Systems Inc. Salem, NH.

References

Baker, T.H.W., Davis, J.L., Hayhoe, H.N., Topp, G.C., 1982. Locating the frozen-unfrozen interface in soils using time-domain reflectometry. Can. Geotech. J. 19 (4), 511–517.

Brown, P.J., DeGaetano, A.T., 2011. A paradox of cooling winter soil surface temperatures in a warming northeastern United States. Agric. For. Meteorol. 151 (7), 947–956.

Campbell, J.L., et al., 2010. Past and projected future changes in snowpack and soil frost at the Hubbard Brook Experimental Forest, New Hampshire, USA. Hydrol. Process. 24 (17), 2465–2480.

Cassidy, N.J., 2009. Electrical and magnetic properties of rocks, soils and fluids. In: Jol, H.M. (Ed.), Ground Penetrating Radar: Theory and Applications. Elsevier, Amsterdam, pp. 41–72.

Christopher, S.F., Shibata, H., Ozawa, M., Nakagawa, Y., Mitchell, M.J., 2008. The effect of soil freezing on N cycling: comparison of two headwater subcatchments with different vegetation and snowpack conditions in the northern Hokkaido Island of Japan. Biogeochemistry 88 (1), 15–30.

Comerford, D.P., et al., 2013. Influence of experimental snow removal on root and canopy physiology of sugar maple trees in a northern hardwood forest. Oecologia 171 (1), 261–269.

Daniels, D.J., 2004. Ground Penetrating Radar. IEE Radar, Sonar, Navigation, and Avionics Series. Institution of Electrical Engineers, London, pp. xxv, 726 pp.

Decker, K.L.M., Wang, D., Waite, C., Scherbatskoy, T., 2003. Snow removal and ambient air temperature effects on forest soil temperatures in Northern Vermont. Soil Sci. Soc. Am. J. 67 (4), 1234–1242.

Doolittle, J.A., et al., 2007. Ground-penetrating radar soil suitability map of the conterminous United States. Geoderma 141 (3–4), 416–421.

Evans, S., 1965. Dielectric properties of ice and snow – a review. J. Glaciol. 5 (42), 773–792.

Fitzhugh, R.D., et al., 2003. Role of soil freezing events in interannual patterns of stream chemistry at the Hubbard Brook experimental forest, New Hampshire. Environ. Sci. Technol. 37 (8), 1575–1580.

French, H.K., Binley, A., Kharkhordin, I., Kulessa, B., Krylov, S.S., 2006. Cold regions hydrogeophysics: physical characterisation and monitoring. In: Vereecken, H., Binley, A., Cassiani, G., Revil, A., Titov, K. (Eds.), Applied Hydrogeophysics. Springer, Dordrecht, Netherlands.

Groffman, P.M., et al., 1999. Snow depth, soil frost and nutrient loss in a northern hardwood forest. Hydrol. Process. 13 (14–15), 2275–2286.

Groffman, P.M., et al., 2001. Colder soils in a warmer world: a snow manipulation study in a northern hardwood forest ecosystem. Biogeochemistry 56 (2), 135–150.

Groffman, P.M., et al., 2011. Snow depth, soil freezing and nitrogen cycling in a northern hardwood forest landscape. Biogeochemistry 102 (1–3), 223–238.

Haei, M., et al., 2011. Effects of soil frost on growth, composition and respiration of the soil microbial decomposer community. Soil Biol. Biochem. 43 (10), 2069–2077.

Hayhoe, H.N., Balchin, D., 1986. Electrical determination for soil frost. Can. Agric. Eng. 28 (2), 77–80.

Henry, H.A.L., 2008. Climate change and soil freezing dynamics: historical trends and projected changes. Clim. Change 87 (3–4), 421–434.

Hentschel, K., et al., 2009. Effects of soil frost on nitrogen net mineralization, soil solution chemistry and seepage losses in a temperate forest soil. Glob. Change Biol. 15 (4), 825–836.

Iwata, Y., Hayashi, M., Suzuki, S., Hirota, T., Hasegawa, S., 2010. Effects of snow cover on soil freezing, water movement, and snowmelt infiltration: a paired plot experiment. Water Resour. Res., 46, 11 pages.

Kaste, O., Austnes, K., Vestgarden, L.S., Wright, R.F., 2008. Manipulation of snow in small headwater catchments at Storgama, Norway: effects on leaching of inorganic nitrogen. Ambio 37 (1), 29–37.

Kopp, M., 1962. Conductivité electriqué de la neige, au courant continu. Z. Angew. Math. Phys. 13 (28), 431–441.

Matzner, E., Borken, W., 2008. Do freeze-thaw events enhance C and N losses from soils of different ecosystems? A review. Eur. J. Soil Sci. 59 (2), 274–284.

McCool, D.K., Molnau, M., 1984. Measurement of frost depth. In: Proceedings of the 52nd Annual Western Snow Conference, Sun Valley, Idaho, pp. 33–42.

Miliken, G., Johnson, D., 1984. Analysis of Messy Data, Volume I: Designed Experiments. Van Nostrand Reinhold Co., New York, pp. 473.

Ricard, J.A., Tobiasson, W., Greatorex, A., 1976. The Field Assembled Frost Gage. Cold Regions Research and Engineering Laboratory, U.S., Army Corps of Engineers, Hanover, New Hampshire.

Saarenketo, T., Scullion, T., 2000. Road evaluation with ground penetrating radar. J. Appl. Geophys. 43 (2–4), 119–138.

Schaberg, P.G., D'Amore, D.V., Hennon, P.E., Holman, J.M., Hawley, G.J., 2011. Do limited cold tolerance and shallow depth of roots contribute to yellow-cedar decline? For. Ecol. Manage. 262 (12), 2142–2150.

Shanley, J.B., Chalmers, A., 1999. The effect of frozen soil on snowmelt runoff at Sleepers River, Vermont. Hydrol. Process. 13 (12–13), 1843–1857.

Steelman, C.M., Endres, A.L., 2009. Evolution of high-frequency ground-penetrating radar direct ground wave propagation during thin frozen soil layer development. Cold Reg. Sci. Technol. 57 (2–3), 116–122.

Steelman, C.M., Endres, A.L., van der Kruk, J., 2010. Field observations of shallow freeze and thaw processes using high-frequency ground-penetrating radar. Hydrol. Process. 24 (14), 2022–2033.

Tierney, G.L., et al., 2001. Soil freezing alters fine root dynamics in a northern hardwood forest. Biogeochemistry 56 (2), 175–190.

Watt, A.D., Maxwell, E.L., 1960. Measured electrical properties of snow and glacial ice. J. Res. Natl. Bur Stand. 64D (4), 357–363.

Yin, X.W., Arp, P.A., 1993. Predicting forest soil temperatures from monthly air-temperature and precipitation records. Can. J. For. Res. 23 (12), 2521–2536.

Zarnoch, S.J., 2009. Testing Hypotheses for Differences Between Linear Regression Lines, e-Research Note SRS-17. U.S. Dept. of Agriculture, Forest Service, Southern Research Station, Asheville, NC, pp. 1, online resource (16 pp.).

Zarnoch, S.J., Dell, T.R., 1985. An evaluation of percentile and maximum likelihood estimators of Weibull parameters. For. Sci. 31 (1), 260–268.